Ecological Applications, 26(3), 2016, pp. 752–770

A characterization of autumn nocturnal migration detected by weather surveillance radars in the northeastern USA

Andrew Farnsworth,[1,5] Benjamin M. Van Doren,[1] Wesley M. Hochachka,[1] Daniel Sheldon,[2,3] Kevin Winner,[2] Jed Irvine,[4] Jeffrey Geevarghese,[2] and Steve Kelling[1]

[1]*Cornell Lab of Ornithology, Cornell University, Ithaca, New York 14850 USA*
[2]*University of Massachusetts Amherst, Amherst, Massachusetts 01003 USA*
[3]*Mount Holyoke College, South Hadley, Massachusetts 01075 USA*
[4]*Oregon State University, Corvallis, Oregon 97331 USA*

Abstract. Billions of birds migrate at night over North America each year. However, few studies have described the phenology of these movements, such as magnitudes, directions, and speeds, for more than one migration season and at regional scales. In this study, we characterize density, direction, and speed of nocturnally migrating birds using data from 13 weather surveillance radars in the autumns of 2010 and 2011 in the northeastern USA. After screening radar data to remove precipitation, we applied a recently developed algorithm for characterizing velocity profiles with previously developed methods to document bird migration. Many hourly radar scans contained windborne "contamination," and these scans also exhibited generally low overall reflectivities. Hourly scans dominated by birds showed nightly and seasonal patterns that differed markedly from those of low reflectivity scans. Bird migration occurred during many nights, but a smaller number of nights with large movements of birds defined regional nocturnal migration. Densities varied by date, time, and location but peaked in the second and third deciles of night during the autumn period when the most birds were migrating. Migration track (the direction to which birds moved) shifted within nights from south-southwesterly to southwesterly during the seasonal migration peaks; this shift was not consistent with a similar shift in wind direction. Migration speeds varied within nights, although not closely with wind speed. Airspeeds increased during the night; groundspeeds were highest between the second and third deciles of night, when the greatest density of birds was migrating. Airspeeds and groundspeeds increased during the fall season, although groundspeeds fluctuated considerably with prevailing winds. Significant positive correlations characterized relationships among bird densities at southern coastal radar stations and northern inland radar stations. The quantitative descriptions of broadscale nocturnal migration patterns presented here will be essential for biological and conservation applications. These descriptions help to define migration phenology in time and space, fill knowledge gaps in avian annual cycles, and are useful for monitoring long-term population trends of migrants. Furthermore, these descriptions will aid in assessing potential risks to migrants, particularly from structures with which birds collide and artificial lighting that disorients migrants.

Key words: BirdCast; nocturnal migration; quantitative description; radar ornithology; spatio-temporal patterns; WSR-88D.

Introduction

Bird migration is one of Earth's amazing spectacles, with billions of birds of many species migrating predominantly at night. Numerous studies have described migratory movements of individual birds (e.g., Bridge et al. 2011, Jahn et al. 2013, McKinnon et al. 2013) or migration densities at a single location (e.g., Gauthreaux 1969, 1971, Erni et al. 2002, Gauthreaux and Livingston 2006). But many fewer studies have detailed nocturnal bird movements at scales that capture population-level movements (Lowery and Newman 1966, Gauthreaux et al. 2003, Buler and Dawson 2014), and even these studies have presented results restricted to a small number of nights or a limited period of night. Studies at these scales are still necessary, primarily to provide data describing fundamental patterns of movement of migrating birds across broad spatial (i.e., continental), temporal (i.e., nightly, seasonal, annual), and population scales. These data are also of practical importance, given the potential impacts of human structures, such as wind turbines and tall, lighted buildings as sources of mortality for nocturnally migrating birds (Kerlinger et al. 2010, Loss et al. 2013, 2014).

Radar is the best source of information to describe nocturnal movements of birds across a range of spatial

Manuscript received 8 January 2015; revised 28 May 2015; accepted 4 August 2015. Corresponding Editor: J. T. Morisette.
[5]E-mail: af27@cornell.edu

TABLE 1. Radar station identifiers, locations, and heights above sea level for 13 WSR-88D stations in the northeastern USA.

Radar station identifier	Nearest city	State	Latitude	Longitude	Height above sea level (m)
KBGM	Binghamton	NY	42.20	−75.98	490
KBOX	Boston	MA	41.96	−71.14	36
KBUF	Buffalo	NY	42.95	−78.74	211
KCBW	Houlton	ME	46.04	−67.81	227
KCCX	State College	PA	40.92	−78.00	733
KCXX	Burlington	VT	44.51	−73.17	97
KDIX	Philadelphia	PA	39.95	−74.41	45
KDOX	Dover	DE	38.83	−75.44	15
KENX	Albany	NY	42.59	−74.06	557
KGYX	Portland	ME	43.89	−70.26	125
KLWX	Sterling	VA	38.98	−77.48	83
KOKX	Brookhaven	NY	40.87	−72.86	26
KTYX	Montague	NY	43.75	−75.68	563

Notes: State abbreviations are NY, New York; MA, Massachusetts; ME, Maine; PA, Pennsylvania; VT, Vermont; DE, Delaware; and VA, Virginia.

scales. For examining migration across broad regions, the appropriate raw data are available from networks of weather surveillance radars, such as the U.S. Weather Surveillance Radar 1988 Doppler or NEXRAD (hereafter WSR-88D; Crum and Alberty 1993, Crum et al. 1993, Doviak and Zrnic 1993). However, challenges in processing the enormous quantity of data that the WSR-88D network captures have constrained its application to a handful of studies (e.g., Gauthreaux et al. 2003, Buler and Diehl 2009, Buler et al. 2012, Buler and Dawson 2014). Furthermore, these challenges are not simple scale-dependent processing issues. The identification of biological targets represented in radar data is difficult. At present, this often requires human expertise, which may not be 100% accurate. Bird movements in the atmosphere rarely occur in isolation in the continental USA; in data representing biological targets, measurements of migrating birds may be confounded with drifting and flying insects and foraging and migrating bats (e.g., Johnson 1969, Russell and Wilson 1997, Russell et al. 1998, Horn and Kunz 2008, McCracken et al. 2008, Chapman et al. 2011). Whereas drifting insects and foraging bats may be more readily identified because their velocities are close to those of winds, flying insects (e.g., large moths and dragonflies) and migrating bats exhibit patterns of nocturnal movement very similar to those of migrating birds (Bruderer and Popa-Lisseanu 2005, Gauthreaux et al. 2008, Alerstam et al. 2011, Krauel et al. 2015).

We examine regional-scale fall migration patterns across the northeastern USA (hereafter NEUS). We identify and describe quantitative and qualitative variation in migration through the night and fall migration season. Our data come from 13 WSR-88D stations in the region from northern Virginia north to the Canadian borders of New York to Maine and for the two fall migration periods of 1 August–30 November in 2010 and 2011. We characterize variation in the density, migration track (i.e., direction to which birds are moving; Alerstam and Hedenström 1998), airspeed, and groundspeed of nocturnal bird migration by date, time, and location at the regional level. We also provide a foundation for expanded use of these data in the future by describing tools to aid and automate the processing of radar data: a new screening tool for rapid review of radar imagery developed by one of the authors and an algorithm to facilitate analysis of WSR-88D velocity data (Sheldon et al. 2013).

METHODS

Input data

We obtained Level II data for 13 WSR-88D stations in the NEUS for all scans between local civil twilight dusk and dawn (i.e., when the sun was at least 6° below horizon) beginning after sunset on 1 August to sunrise on 1 December for 2010 and 2011 from the National Climatic Data Center (*available online;* Table 1).[6] We restricted our analysis to this range of times because sunset and sunrise scans are dominated by diurnal and stopover activity, including birds and other biological targets (e.g., diurnal and crepuscular insects; Chapman et al. 2011) not necessarily engaged in nocturnal flights. Level II data consist of basic products, of which we used base reflectivity and radial velocity. Every 6–10 min, each radar antenna scans a volume of the atmosphere by sending pulses of microwave energy outward in a predefined scanning pattern (Crum and Alberty 1993, Crum et al. 1993). The reflections of these pulses from objects (i.e., birds, insects, hydrometeors) are summarized within volumes of space, termed "pulse volumes" (PV; also known as sample volumes), determined by the width of

[6]http://www.ncdc.noaa.gov/nexradinv/

a radar's beam and that radar's resolution in radial distance along the beam (0.5° wide and 250 m long for this study's radars). Absolute PV size increases with distance from the radar, and PVs represent "the smallest quantifiable measure of reflectivity or velocity" using Level II data (Larkin and Diehl 2012). Our data consisted of one scan (i.e., a single execution of the scanning pattern) per hour per station, starting with the scan closest to local sunset and continuing in approximately 1-h increments until local sunrise, with scans no more than 5 min from the desired hourly interval (n = 39840 hourly scans in total).

We analyzed radar reflectivity data from all PVs within 37.5 km of each radar station up to a sampling height of 3000 m above the radar station in 30 100-m intervals (hereafter bins). We used standard assumptions about atmospheric refraction and beam propagation (the 4/3 Earth radius model; Doviak and Zrnic 1993) to compute PV height from antenna angle and distance from the radar. We used a 3000 m cutoff based largely on previous work suggesting this altitude was an upper limit that encompassed most migration in this region (Williams and Williams 1978). The primary rationale (e.g., from Buler and Diehl 2009, Dokter et al. 2011) for analyzing data from this small (37.5 km radius, 3 km height) region relative to the entire range is to work within the volume of atmosphere with the most accurate estimates of radar beam height and to minimize use of data from pulse volumes experiencing non-standard refraction of the radar beam (e.g., anomalous propagation, spurious patterns caused by interactions with thermal inversion layers and other varying atmospheric phenomena; Bech et al. 2012).

Reflections returned to and received by a radar antenna (i.e., "returns") represent either targets of potential interest or "clutter" caused by objects on or near the ground. PVs vary slightly in their spatial positions among and within scans for several reasons, including (1) variations in PV resolution across different data products (reflectivity and radial velocity) within a single scan, (2) variations in PV resolution across radar operating modes, and (3) variability in the physical movement of the antenna from scan to scan. To facilitate analyses that compare a specific volume in space across multiple data products or scans, we aligned the edges of all PVs to a fixed polar grid with angular resolution of 0.5° and 250 m range bins by applying nearest neighbor interpolation.

We visually screened all hourly radar scans using a custom-designed web application (Irvine 2013). We excluded scans that contained precipitation or ground clutter due to anomalous propagation within 37.5 km of the radar station. Two of us (A. Farnsworth and B. Van Doren) manually classified each scan as either "accept" (scan was free of precipitation within 37.5 km of the radar) or "reject." We achieved a review rate of one scan every 2–3 s. Agreement in classification between A. Farnsworth and B. Van Doren was 97.27% (i.e., 38751 out of 39840 scans were given the same labels). Retaining only accepted scans from both reviewers yielded our filtered dataset of 27850 scans.

We processed the radar data using MATLAB (MATLAB and Statistics Toolbox Release 2013*b*) scripts and RSL, the radar software library written in C (Wolff 2009) to format the data for use within MATLAB.

Identifying confounding sources of radar reflections

We excluded PVs with consistently high returns from targets on or near the ground that were not already filtered in the Level II data (static clutter maps; after Buler and Diehl 2009). We did this using the fixed polar grid described previously, which allowed us to match pulse-volumes directly between sweeps, and for scan elevation angles of 0.5°, 1.5°, 2.5°, 3.5°, and 4.5°, elevations typical of volume coverage patterns (VCP) for WSR-88D (Warning Decision Training Branch 2008). For each PV, we analyzed its associated returns' probability of detection (POD) and mean reflectivity over the entire set of scans (Buler and Diehl 2009). POD is defined as the proportion of reflectivity measurements that exceeded a fixed threshold, which we set to 10 dBZ. We classified PVs with POD at least 0.7 and mean reflectivity across all scans at least 15 dBZ as ground clutter. Visual inspection of radar images confirmed that this rule captured ground clutter but did not filter out other PVs.

We also looked for the potential issue of occultation, in which the radar beam would be partly or mostly blocked from reaching more distant PVs by fixed structures (e.g., mountains, buildings) close to the radar. Since we limited ourselves to analyzing radar returns within 37.5 km of stations and the analysis region is not very mountainous, the impact of beam blockage was extremely limited at all stations except KCXX in Burlington, Vermont, USA. From visual inspection of this station's imagery, 30–50% of PVs at the lowest elevation angle were partly or completely blocked. The overall impact of including these PVs was mitigated because we used data from five elevation angles in each set of scans, and beam blockage was only significant at the lowest angle.

Excluding additional, variable clutter from targets on or near the ground is a common radar analysis practice (Doviak and Zrnic 1993), and we classified all PVs with radial velocity measurements in the range ± 1 m/s as "dynamic clutter" and excluded them from analysis. This is a conservative rule and also excluded airborne targets moving orthogonally to the direction of propagation of the radar beam; however, these excluded PVs represented a negligible fraction of all targets.

Velocity profiles

We created velocity profiles, representations of targets' direction and speed by height, from raw radar data as the basis for calculating targets' movements in the aerosphere. We calculated mean velocities of targets at different elevations using a novel algorithm developed as part of the BirdCast project (Sheldon et al. 2013) and

built on a set of techniques known as velocity-azimuthal display (VAD) or velocity volume profiling (VVP; Doviak and Zrnic 1993), methods that fit regression models to observed winds. Sheldon et al. (2013) extended these methods by incorporating a model for aliasing. Aliasing is the ambiguity in radial velocity measurements caused by targets exceeding a radar's maximum velocity measurement (i.e., Nyquist value, a function of pulse interval and radar wavelength). It manifests most frequently in Level II data as PVs whose apparent velocity has the opposite sign of the true velocity (e.g., targets appear to be approaching the radar when they are actually moving away from the radar). More specifically, the true radial velocity is shifted by an unknown multiple of twice the Nyquist value until its absolute value is smaller than the Nyquist value. Unlike most previous approaches to VAD, the Sheldon et al. (2013) algorithm performs velocity profiling using raw radial velocity data that retain aliasing. In using this algorithm, we assigned PVs to a single 100 m height bin based on the center of the PV and extracted for each bin (1) mean target velocity, which is the estimated mean velocity in a uniform velocity model (i.e., assumption that targets at each elevation have a common mean velocity that is perturbed by Gaussian noise for each 100 m height bin; Doviak and Zrnic 1993); (2) root-mean-square error (RMSE) of the actual radial velocity measurements relative to the estimated mean velocity; and (3) number of PVs in the height bin.

Density calculation

To distinguish birds from windborne targets (e.g., dust, smoke, and some insects), we compared the radial velocity of each PV to the radial component of wind velocity at the same location to determine radial airspeed, which is the component of the airspeed vector (target velocity minus wind velocity) along the direction of the radar beam (Gauthreaux et al. 2003). This value does not exceed true airspeed, is equal to true airspeed for targets moving directly toward or away from the radar, and is very close to true airspeed for targets with little motion tangential to the radar beam (e.g. Gauthreaux and Belser 1998). For our purposes, we excluded all data from targets traveling more than 15° from the primary direction of movement derived from each height bin's velocity profile. We obtained data on radial wind velocity from the North American Regional Reanalysis (NARR) project (Mesinger et al. 2006). NARR data files are available at 3-h increments and report weather variables on a three-dimensional grid with points spaced approximately 32 km apart in the *x*- and *y*-directions, using pressure instead of height as the *z*-direction. We converted 29 pressure levels (in hPa) approximately covering the lowest 15000 m of the atmosphere above the ground to heights based on a National Weather Service table that also uses the U.S. Standard Atmosphere definition (Krueger and Minzner 1976, U.S. Standard Atmosphere 1976), using only those converted heights covering 0–3000 m above sea level (i.e., pressure levels from 700 to 1000 hPa). The NARR estimates are based on measurements from many different sources; they are not the product of instantaneous measurements taken at each grid point (e.g., unlike radiosonde data from Gauthreaux et al. 2003). We computed radial wind velocity for each PV by extracting the full record of wind velocity and direction from the closest NARR grid point and computing the component of velocity that was in the direction of the beam. We retrieved and averaged wind values for each PV from NARR data using a simple nearest neighbor interpolation scheme based on the NARR estimate closest in time to the scan time and the NARR three-dimensional grid point closest to the PV location. If the mean radial airspeed of targets in a PV was <5 m/s (i.e., likely dominated by windborne targets; e.g., Larkin 1991, Gauthreaux and Belser 1998, Gauthreaux et al. 2003, Buler and Dawson 2014), we classified the PV as dominated by windborne targets and set that PV's reflectivity to zero. Briefly, we found that setting these volumes to missing increased average densities, whereas setting them to zero decreased densities. Despite this choice between imperfect options, we chose the latter as it is more conservative (for greater detail, see Appendix S1: Fig. S1). We also considered PVs with no data (i.e., signal-to-noise ratio below the minimum threshold determined by WSR-88D) as having reflectivities of zero and discarded from our analysis PVs classified as static or dynamic clutter, in addition to the previous exclusion of data beyond 15° from the primary direction of target movement. From the remaining PVs, we discarded the largest and smallest 25% of all values, as well as any values exceeding 35 dBZ, to minimize the potential impact of false zeros due to suppressed clutter in the Level II data and very high reflectivity values due to undetected clutter (Buler and Diehl 2009).

We computed bird density in each of the 30 100-m height bins for 0–3000 m above the radar station by averaging each bin's reflectivity values for PVs within 15° of the primary axis of movement, with height bins contributing in proportion to their volumes regardless of the number of PVs remaining in the bin after classification. We assumed that the remaining PVs were representative of the density in that height bin. We converted from WSR-88D units of reflectivity factor (Z, mm^6/m^3) to reflectivity (η, cm^2/km^3), the total effective scattering area of targets per unit volume (Chilson et al. 2012*b*), and then added the values from each elevation bin and multiplied by bin height to get the per-scan total reflectivity (units cm^2/km^2), or the total effective scattering area of all targets within 0–3000 m elevation/km^2 of Earth's surface, hereafter referred to as bird density. For each scan, we also computed average airspeed and groundspeed over the entire scan as the reflectivity-weighted mean of airspeed and groundspeed from each elevation bin and the per-scan average migration track as the reflectivity-weighted circular mean of migration

tracks from each elevation bin. We excluded from the average any information from elevation bins in which the velocity measurements were based on fewer than 10 PVs or where the RMSE was more than 5 m/s.

Statistical modeling of within-night variation

Bird migration may vary within a night and among stations, with the potential to make description of whole-night migration patterns challenging. Therefore, our first step in describing any facet of migration (i.e., density, direction airspeed, and groundspeed) was to statistically model patterns of variation within each night. To account for seasonal and geographic variation in duration of the nocturnal period, we standardized times of night by dividing each time by the night's duration. Thus, we assigned each scan a time between 0 and 1, with 0 indicating the start of civil twilight and 1 indicating the end. This approach facilitated direct comparison more easily than using absolute time. For some analyses, we divided this continuous period into deciles. We constructed generalized additive mixed models in which migration could potentially vary jointly with the smoothed tensor product (Wood 2006) of (1) standardized time of night (continuous variable from 0 to 1) and (2) Julian day of the year (continuous variable). We modeled these predictors as smooth terms to avoid imposing any a priori constraints, since we expected migration might vary with time in a nonlinear manner. We used a tensor product because our two predictor variables were on different scales (Wood 2006: p. 162). We also included radar station and the night of observation as random intercept effects, in order to account for non-independence among scans from the same station and from the same night.

For within-night statistical models, our goal was to describe patterns of relative change within the night irrespective of night-to-night variation in absolute values of the response. We therefore standardized values of density by dividing the measured density of each scan by the maximum density for that station-night. We standardized airspeed, groundspeed, and wind speed at 925 hPa (an appropriate height for nocturnal passerine migration; e.g., Dokter et al. 2011, Kemp et al. 2013) by dividing these numbers by the appropriate density-weighted average value for that station-night. We calculated standardized direction of each scan by subtracting the density-weighted average direction for that station-night, thereby describing the direction of each scan relative to that of the "average bird." We applied a similar procedure to standardize wind directions at 925 hPa, except we used wind speed as the weighting variable. We did not standardize directions by division because the circular nature of the data and the lack of absolute units would not yield easily interpretable results. As a result, interpretations of models describing within-night variation in direction of travel need to account for the existence of variation in the average direction of travel from night to night. For all data types, we only included nights with radar data for at least the third and fourth deciles of night (i.e., the period with the highest migrant densities aloft; see *Results*). This improved within-night standardization and ensured that nightly averages (see *Statistical modeling of among-night variation*) included the most important times of night.

We also needed to account for the potential imperfect filtering of windborne returns from bird returns in our density computations. Even though this filtering removed data that were not describing bird movements, we presumed that some windborne targets remained in all hourly scans we deemed to contain birds. We made two assumptions: first, these windborne targets represented ever-present background noise, and second, estimates of speed and direction would be more accurate when large numbers of birds were aloft (i.e., a higher bird signal to windborne noise ratio). To minimize the remaining effects of windborne contamination not addressed by filtering, we weighted the data points in our statistical models describing variation in migration speed and direction by density of birds (cm^2/km^2) in the air. We did not weight data in models describing variation in density. We fit all models using the gamm function (package mgcv; Wood 2011) in R (version 3.1.2; R Core Team 2014).

In all cases, we verified that model residuals were symmetrically distributed. For models describing variation in bird density, we log-transformed the response variable to satisfy residual symmetry. We quantified goodness of fit for each model by comparing predicted values to observed data and calculating the coefficient of determination (hereafter R^2*), weighting the relationship when appropriate.

We report descriptions of central tendency and dispersion as mean ± 1 SE for densities, airspeeds, and groundspeeds. For migration tracks, we report circular means weighted by bird density with bootstrapped 95% confidence intervals (10000 iterations; hereafter CI). We used bootstrapped CIs because these intervals were often asymmetric, making standard formulae for calculating confidence intervals inappropriate.

To evaluate the impact of our wind-based thresholding procedure, we compared the mean directions of two groups of scans using a permutation test: we simulated the null hypothesis of no difference between groups by comparing the actual difference in means to the distribution of 10000 randomly sampled differences in means. The calculated P value is the proportion of times a randomly sampled value is at least as extreme as the actual value.

Statistical modeling of among-night variation

From our analyses of within-night variation we created response variables summarizing migration and wind (i.e., bird density, migration direction, wind direction, airspeed, groundspeed, and wind speed) for each night. We modeled these nightly response values, in this case unstandardized to reflect night-to-night variation, using

a similar statistical approach as outlined above. We did not use tensor products because we had only one main predictor: day of year (DOY). This predictor was included as a smooth term, and we included station as a random intercept effect. We calculated response values representing whole-night migration as follows. For a given night, we chose the hourly scan with the highest bird density as the nightly measure of reference for bird density. Our nightly measure of migration track was a bird density-weighted circular mean of hourly scan data for a given night. We applied a similar procedure for wind direction, weighting by wind speed. Our nightly measures airspeed, groundspeed, and windspeed were density-weighted averages of these speeds for each night. For migration track, airspeed, and groundspeed, weighting by density resulted in a model that reflected the behavior of the greatest densities of birds.

We conducted a final analysis designed specifically to identify correlations in flight densities among radar stations. We quantified the similarity of peak migrant densities between all pairs of stations by calculating the Spearman rank correlations of nightly mean bird densities during nights of substantial migration. We accounted for multiple comparisons using the Benjamini–Hochberg procedure to adjust *P* values (Benjamini and Hochberg 1995). We define these nights of region-wide substantial migration as nights on which mean bird density across all stations exceeded scans' 90th percentile. Maximum densities, as used in other analyses, would not suffice for this analysis because a high maximum density could represent a local movement at a single station instead of a regional movement across all stations. Therefore, in choosing mean density over maximum density as a metric for including nights of substantial movements, we chose to investigate nights with large and widespread movement as opposed to nights when movement may have been large but also geographically limited in scope. Fifty-nine nights with high densities of migrants were selected by choosing only data from the nights with the top 10% of migrant densities.

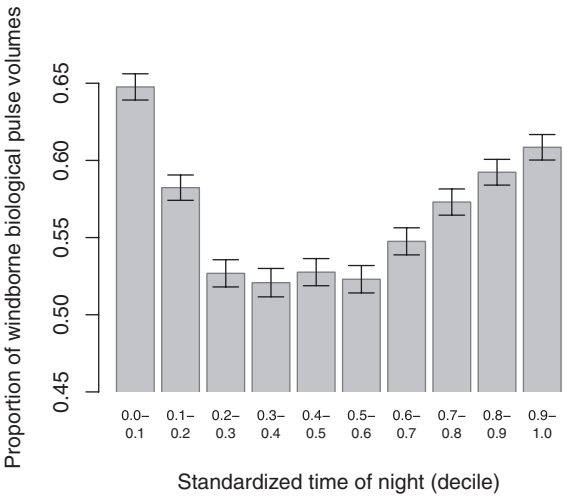

FIG. 1. Proportion of biological pulse volumes classified as windborne from 13 WSR-88D stations in the northeastern USA by decile of the night. Each column represents the mean ± 1 SE for pooled 2010 and 2011 data for all nights for all stations for each decile.

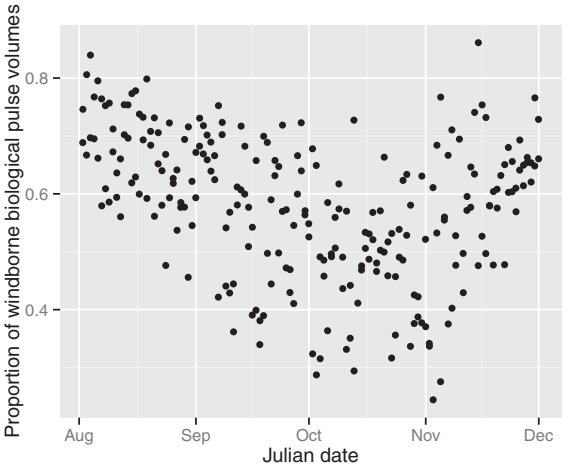

FIG. 2. Proportion of biological pulse volumes classified as windborne from 13 WSR-88D stations in the northeastern USA by Julian day. Each point represents the mean for pooled 2010 and 2011 data for all radar stations for each night.

RESULTS

Removal of windborne targets

In most scans, PVs dominated by putative windborne targets represented a substantial proportion of scan's total PVs, with proportions of these windborne targets peaking in the first decile of night (Fig. 1). We also found the highest proportions of windborne PVs to occur early and late in the fall (Fig. 2). This pattern of windborne PVs exhibited a distinctly different pattern than bird migration (see section below on within night variation in patterns of bird migration). Our PV screening to address low reflectivity scans containing the highest proportions of windborne PVs (Fig. 3) removed much (but not all) windborne signal found in our dataset (see Appendix S1: Fig. S1).

Following screening to remove windborne targets, the remaining data showed the average directions of travel to be more consistent with expectations of migrating birds' directions (Fig. 4). Based on past studies in the region (e.g., Drury and Keith 1977, Williams et al. 1977, Williams et al. 2001), mean direction of travel of birds should be toward south-southwest, whereas data without thresholding or weighting by bird density showed targets on average traveling to the southeast (162.62°; Fig. 4A). A southeasterly direction of movement is consistent with the direction of prevailing winds, strongly suggesting that the raw data (i.e., before thresholding) were influenced by windborne targets. Thresholding by itself created a subset of data in which targets typically traveled almost due south (181.01°; Fig. 4B), although many targets

traveling to the southeast and east still remained. We believe this bimodal distribution represents the different directions of targets that are windborne (e.g., drifting insects and foraging bats) and non-windborne (i.e., birds and some bats). Weighting observations by bird density resulted in a calculated mean direction of travel across all data that was more consistent with expectation (205.31°; Fig. 4C). This mean direction was significantly different after both thresholding and weighting (209.28°; Fig. 4D; $P = 0$, permutation test). Applying our thresholding step before weighting had even more dramatic results across smaller subsets of data (Appendix S1: Fig. S2).

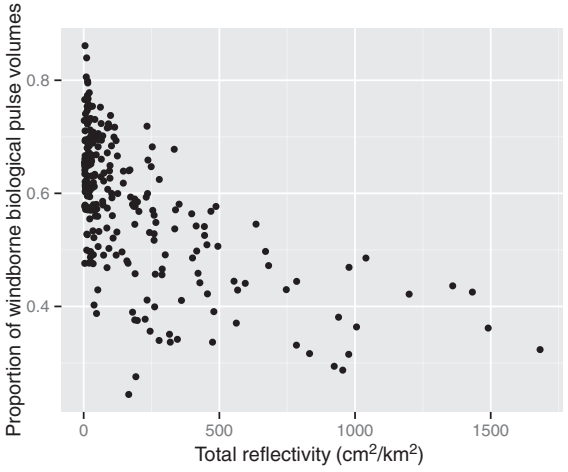

FIG. 3. Proportion of biological pulse volumes classified as windborne on mean total reflectivity from 13 WSR-88D stations in the northeastern USA. Each point represents the nightly mean for 2010 and 2011 for all radar stations.

Looking beyond average directions, weighting and thresholding also reduced the frequency of individual observations of seasonally less appropriate or inappropriate directions for bird migration: targets that were being carried by the primarily southerly winds from 90° to 270° (Fig. 4A, B). Weighting by bird density further de-emphasized data from targets in this directional range (Fig. 4C, D). However, whereas thresholding and weighting largely removed information about windborne targets from the data, we also suspect that some information from slower-flying birds was either removed or down-weighted in the process.

Following thresholding to remove pulse volumes from the original data and weighted averaging, mean direction of movement was 209.28° and did not differ between years (2010, 209.85°; 2011, 208.47°; $P = 0.15$, permutation test). Mean airspeeds and groundspeeds of migrating birds were 7.10 m/s and 10.65 m/s, respectively.

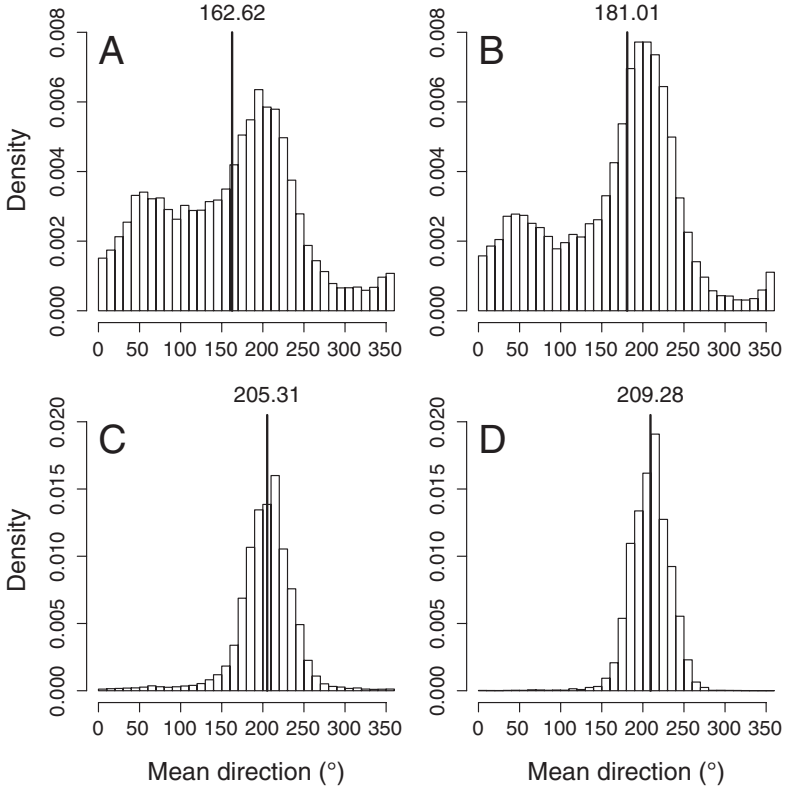

FIG. 4. Frequency distribution of mean directions of radar targets before and after thresholding and before and after weighting directions by bird density for 13 WSR-88D stations in the northeastern USA. Panels show (A) no thresholding, no weighting; (B) thresholding, no weighting; (C) no thresholding, weighting; and (D) thresholding, weighting.

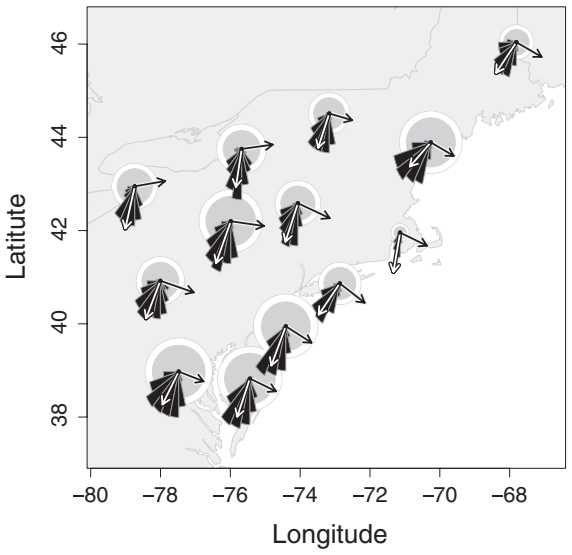

FIG. 5. Mean density, track, and groundspeeds of bird targets from 13 WSR-88D stations in the northeastern USA for 2010 and 2011. Radii of gray circles are proportional to the square root of mean density in cm^2/km^3 with standard errors as white boundaries; white arrows represent bird density-weighted ground headings of bird targets, scaled by ground speeds; histograms in dark gray represent the frequency distributions of these weighted tracks. Dark gray arrows represent wind directions, scaled by wind speed.

Some bird migration occurred almost every night of the fall (average density, 95.06 ± 2.07 cm^2/km^3), but large movements occurred relatively infrequently (Appendix S1: Fig. S3). Figure 5 presents a graphic summary of these means and variation around them.

Within-night variation in patterns of bird migration

Our analyses indicate that systematic variation occurred in nightly patterns of bird density, direction, and speed of nocturnally migrating birds (see Tables 2 and 3 for a summary). In general, these within-night patterns showed little variation (i.e., narrower confidence intervals) during the middle of the season, when bird densities peaked, in contrast to substantially greater within-night variation at the beginning and end of the season when bird densities were much lower. Nightly bird densities peaked in the first half of the night (third–fifth deciles; Fig. 6). Direction of travel also exhibited systematic variation through the night, with a positive (i.e., clockwise) shift in track from south-southwesterly to southwesterly particularly evident mid-season (Fig. 6). Groundspeeds were generally highest early in the night (third and fourth deciles) until late in the season, when they were highest just after nightfall (Fig. 6; dotted lines). Airspeeds were generally lowest at the start of the night, especially mid-season, but increased rapidly towards the end of the night late in the season (Fig. 6; solid lines). Winds on average originated from the northwest (see Fig. 5; black arrows) and exhibited the greatest positive (clockwise) nightly shifts in September and October, but with magnitudes of only 15° or less. Wind speeds generally decreased during the night, with the exception of November, when the minimum occurred in the middle of the night (Fig. 6; dashed lines).

Among-night variation in patterns of bird migration

Systematic differences in migratory patterns were apparent both across the region and through the season at individual sites (Tables 2 and 3). The lowest maximum bird densities occurred at Boston, Massachusetts, USA; the highest occurred at Dover, Delaware, USA. Nightly bird density peaked in late September, with the greatest overall densities occurring between mid-September and mid-October (Fig. 7). Density-weighted nightly migration tracks during this period generally varied little, averaging between south-southeast and south-southwest. An easterly shift occurred towards the end of the season (Fig. 8), but bird densities were very low during this period (Fig. 7), suggesting other influences might be driving this pattern. Within this general pattern, we also found systematic variation among stations: mean tracks ranged from the most southwesterly at Portland, Maine (229.29°) to primarily southerly or south-southwesterly at Boston, Massachusetts (192.79°), Buffalo, New York (196.68°), Montague, New York (191.49°), and Burlington, Vermont, USA (203.40°; Table 2). Mean density-weighted groundspeeds varied greatly over the fall season in concert with shifts in wind direction (and therefore strength of tailwinds), but showed an increasing trend (Fig. 8). Groundspeeds were highest at Binghamton, New York and lowest at Portland, Maine, USA (Table 2). We also found a seasonal increase in airspeed (Fig. 8); an end of the season decrease occurred during the same period as the previously discussed easterly shift, when bird densities were very low. Table 2 reports the mean and dispersion for migration metrics by station. Wind direction varied substantially during the season, but differed from migration tracks by at least 30° and as much as 100°; wind speeds were similar in magnitude to airspeeds, generally increasing during the season (Fig. 8).

Regional correlation in bird density among radar stations

The above results indicate that migration varies systematically with time of night, day of year, and location across the study region. Our final analysis showed that, in terms of geographical variation in migration intensity, the NEUS can be divided into two sub-regions. For nights of substantial bird migration, we found the greatest correlation in bird density among the region's northern inland and southern coastal stations (Fig. 8). Interestingly, we found that these two sub-regions were not connected by strong or significant correlations, with a noticeable lack of correlation or connection between Portland, Maine, and Boston, Massachusetts, and additional stations to the southwest across most of the NEUS.

Table 2. Summaries of nocturnal migration characteristics for 13 WSR-88D in the northeastern USA.

Class	Identifier	Bird density	Bird density SE	Density-weighted mean migration track	95% CI, low migration track	95% CI, high migration track
Decile	0 (0.0–0.1)	49.37	4.15	200.05	196.68	203.41
	1 (0.1–0.2)	92.50	5.54	203.50	200.90	206.18
	2 (0.2–0.3)	162.18	8.23	204.65	202.51	206.78
	3 (0.3–0.4)	183.91	9.80	206.03	203.93	208.13
	4 (0.4–0.5)	142.69	8.17	209.06	206.73	211.37
	5 (0.5–0.6)	116.15	7.31	212.98	210.49	215.47
	6 (0.6–0.7)	91.02	6.66	214.87	212.32	217.43
	7 (0.7–0.8)	57.76	4.92	218.76	215.43	222.07
	8 (0.8–0.9)	37.72	3.66	224.80	221.09	228.57
	9 (0.9–1.0)	15.37	1.92	227.69	223.01	232.42
Radar station	KBGM	145.77	8.80	205.31	203.17	207.36
	KBOX	8.98	1.01	192.79	189.09	196.62
	KBUF	73.33	4.93	196.68	194.11	199.34
	KCBW	38.51	3.35	221.52	217.72	225.10
	KCCX	79.80	5.85	207.03	203.12	211.24
	KCXX	57.74	4.61	203.40	200.05	206.75
	KDIX	140.45	11.70	206.35	204.23	208.56
	KDOX	151.25	8.80	203.93	201.98	206.05
	KENX	69.15	5.51	203.40	200.73	205.84
	KGYX	141.90	8.71	229.29	227.25	231.42
	KLWX	164.31	9.84	213.53	210.61	216.60
	KOKX	60.52	4.71	222.20	220.36	223.93
	KTYX	80.66	7.53	191.49	188.59	194.08

Class	Mean groundspeed	Groundspeed SE	Mean airspeed	Airspeed SE	Number of scans	Number of nights
Decile	10.29	0.11	6.62	0.06	2201	243
	10.70	0.10	7.27	0.06	2695	241
	10.75	0.10	7.56	0.06	2557	241
	10.94	0.11	7.43	0.06	2357	240
	11.05	0.11	7.48	0.06	2519	239
	10.95	0.11	7.32	0.06	2437	240
	10.66	0.11	7.17	0.06	2403	241
	10.59	0.10	6.98	0.06	2566	242
	10.33	0.10	6.58	0.06	2478	241
	10.01	0.10	6.34	0.06	2478	242
Radar station	11.89	0.11	8.04	0.08	1922	217
	10.33	0.12	5.84	0.06	2037	226
	11.30	0.11	7.42	0.08	1765	212
	10.50	0.13	6.98	0.08	1765	211
	10.83	0.13	7.48	0.07	1878	217
	9.61	0.10	6.98	0.07	1738	214
	11.27	0.13	7.06	0.07	2069	227
	10.73	0.12	6.64	0.07	2049	224
	10.82	0.12	6.95	0.06	1818	211
	9.54	0.11	7.71	0.07	1944	219
	10.15	0.11	7.34	0.06	2139	227
	10.84	0.12	6.56	0.07	1997	222
	9.99	0.12	7.08	0.08	1570	198

Discussion

We took a conservative approach to measuring bird migration with WSR-88D radar. This involved visually pre-screening radar images to exclude precipitation and other clutter, thresholding to remove pulse volumes that did not fit certain criteria and may have represented windborne targets, and weighting statistical

TABLE 3. Summary of GAMM model results for nightly and seasonal density, track and speed of birds, and direction and speed of winds.

Response variable	Scope	Effective df	F	P	R^2
Migration track	within-night	18.1	427.1	<0.0001	0.265
	across-season	8.0	7.9	<0.0001	0.022
Bird density	within-night	22.3	253.4	<0.0001	0.230
	across-season	7.0	180.3	<0.0001	0.291
Groundspeed	within-night	19.1	23.1	<0.0001	0.028
	across-season	8.9	96.5	<0.0001	0.253
Airspeed	within-night	19.4	35.7	<0.0001	0.042
	across-season	8.3	123.4	<0.0001	0.292
Wind speed	within-night	18.4	17.5	<0.0001	0.016
	across-season	1.0	322.7	<0.0001	0.101
Wind direction	within-night	10.9	8.3	<0.0001	0.003
	across-season	8.6	9.7	<0.0001	0.041

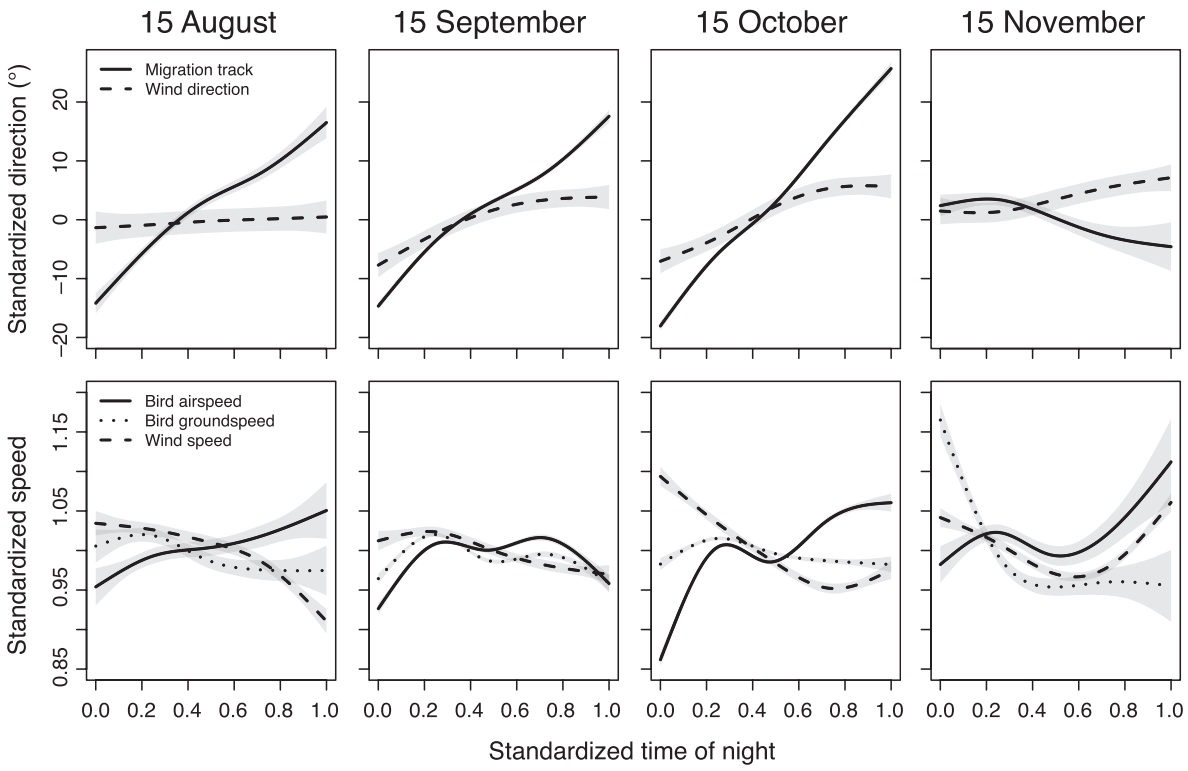

FIG. 6. Examples of within-night variation in the direction and speed of migration by standardized time of night for 13 WSR-88D stations in the northeastern USA for 15 August, 15 September, 15 October, and 15 November. Data are pooled 2010–2011. Top row, mean ground headings in degrees for birds standardized by subtracting the density-weighted, within-night average direction for birds (solid line) and for wind (dashed line); bottom row, mean groundspeeds standardized by density-weighted, within-night average groundspeed (dotted line), mean airspeeds standardized by density-weighted, within-night average airspeed (solid line), and mean wind speed (dashed line). Gray shading is 1 SE from the mean.

analyses to emphasize data from times of high migrant densities. Although we could not remove all windborne targets, our results suggest that our methods are effective at reducing the impact of windborne targets and produce final patterns that are consistent with literature and expectations for migrating birds. They provide confidence that we can effectively extract migration signal from these radar data. Qualitatively, the patterns of migration that we observed were similar across the region: the primary axis of movement was overland to the south-southwest, especially on the nights with the highest densities of migrating birds, and

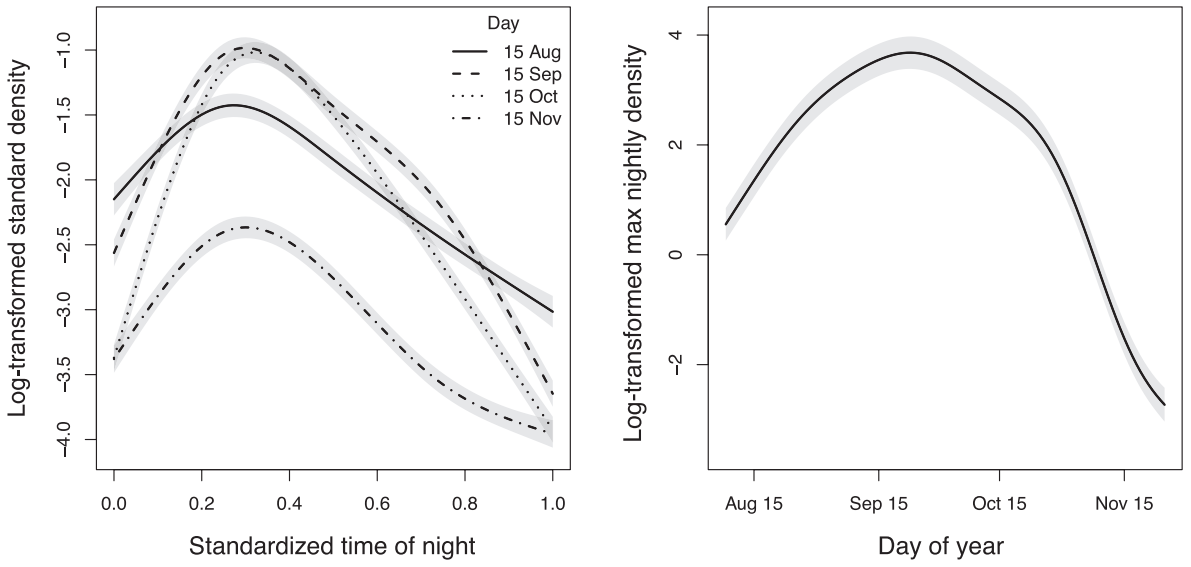

FIG. 7. Patterns of log-transformed mean bird density for 13 WSR-88D stations in the northeastern USA. Left, pooled 2010–2011 nightly mean bird density for 15 August (solid line), 15 September (dashed line), 15 October (dotted line), and 15 November (dot and dash line); right, pooled 2010–2011 seasonal mean bird density. Gray shading is 1 SE from the mean.

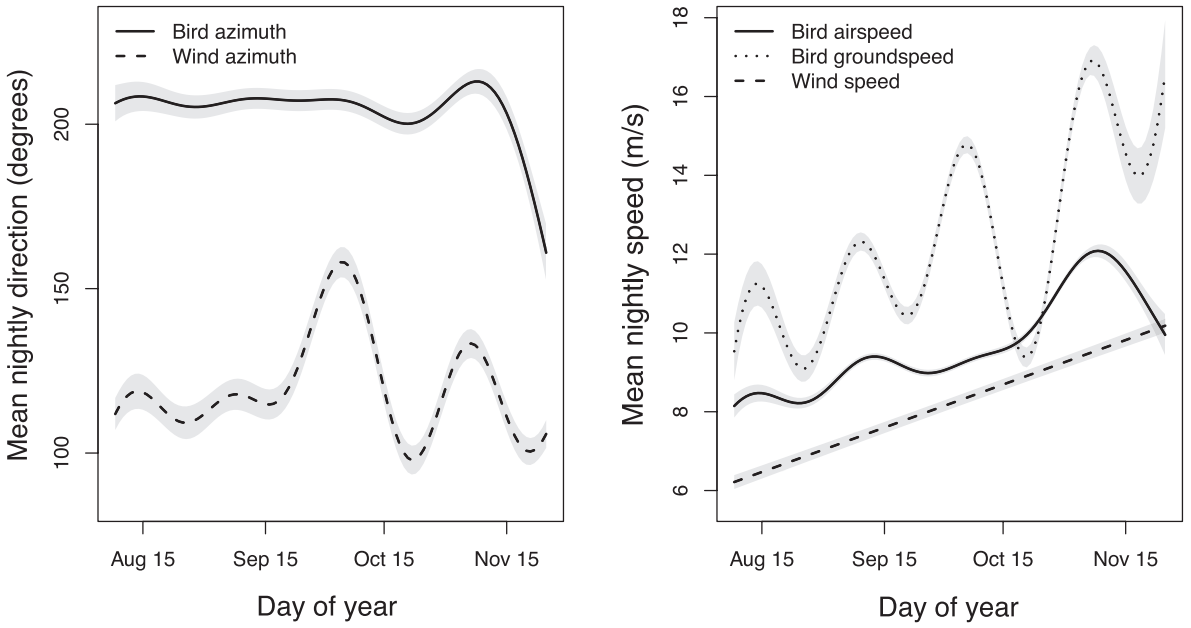

FIG. 8. Seasonal variation in the direction and speed of migration for 13 WSR-88D stations in the northeastern USA. Data are pooled 2010–2011. Left, mean ground headings weighted by bird density (solid line) and mean wind heading (dashed line); right, mean groundspeeds weighted by bird density (dotted line), mean airspeeds weighted by bird density (solid line), and mean wind speed (dashed line). Gray shading is 1 SE from the mean.

airspeeds and groundspeeds of migrating birds generally increased over the course of the fall. Migration patterns, most notably densities of birds overhead, varied systematically within nights and across the fall season.

For all of these characterizations of migration activity, we have less precision in describing patterns early and late in the fall season. Given the smaller densities of birds early and late in the season, and typical lower weighing of data from the start and end of the fall season, we cannot determine whether this greater variability is biological or an artifact of the predicted patterns being driven largely by the more highly weighted data from the middle of the fall.

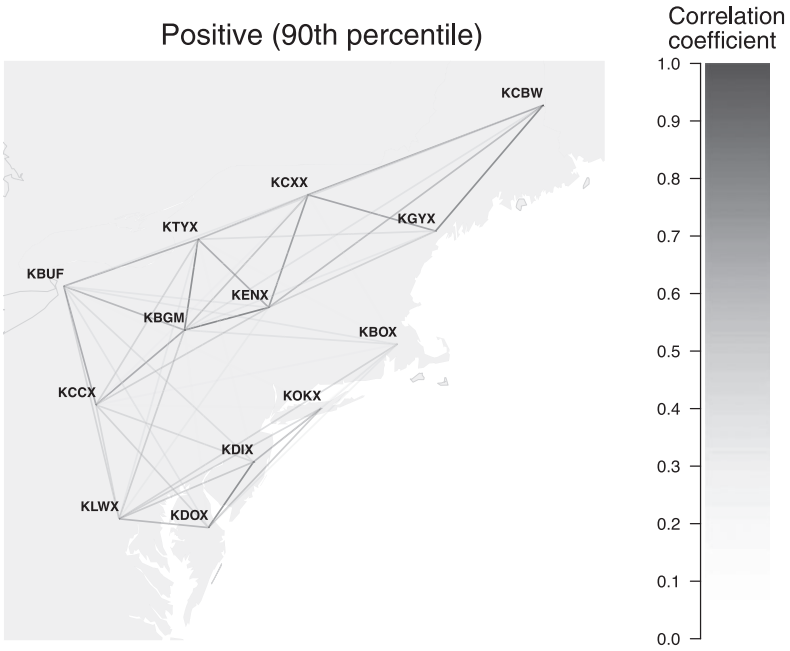

FIG. 9. Spearman rank correlations in mean bird density at or above the 90th percentile among 13 WSR-88D stations in the northeastern USA. Darker colors and solid lines connect stations with stronger, statistically significant positive correlations.

Birds vs. windborne targets

Windborne contamination is frequent in the pulse volumes of nocturnal weather surveillance radar scans, even when volumes containing precipitation are excluded. Our results suggest that such targets were present in many hourly scans in our dataset and dominated those with low overall reflectivity. This stood in contrast to scans with the largest mean reflectivities (uncorrected for windborne targets; Fig. 3), where we believe bird targets dominated. Windborne targets early in the fall (e.g., August) likely include insects and some foraging bats (Gauthreaux et al. 2008), but the composition of windborne targets later in the season (e.g., November) is unclear. Radar detection of insects (Chapman et al. 2011, Westbrook et al. 2013, Drake 2014), dust and particulate matter (Jones and Christopher 2009, Jones et al. 2009), and bats (Horn and Kunz 2008, Frick et al. 2012) is well documented. Dust, particulate matter, and most insects will be categorized as windborne by our airspeed criteria. Depending on their mode of flight, bats might be classified as windborne (e.g., foraging flight) or bird (e.g., consistent flight in a linear direction within a single pulse volume). However, bats are likely to represent only a small portion of the targets we classified as birds.

Our results suggest that airspeed-based classification is useful for reducing the number of windborne targets that are considered as birds. In particular, PVs classified as windborne were much more likely to have very low reflectivity values (Appendix S1: Figure S1; similar pattern at the whole-scan level; Fig. 3), which is consistent with returns from dust or insects. Filtering windborne PVs (with or without weighting by density) led to much more appropriate measurements of migration direction (Fig. 4), which lends additional credence to the classification. However, it is inevitable that some PVs were misclassified by the airspeed criteria. Several factors can lead to misclassification. First, airspeed estimates may be inaccurate due to local-scale differences in actual wind velocity from coarse-resolution NARR estimates. Second, even if individual birds fly with airspeed faster than 5 m/s, the average airspeed measured across an entire PV will be lower if it contains birds flying in many directions. Third, the 5 m/s threshold will misclassify some targets whose airspeeds do not match this assumption, such as fast-flying insects or bats, or slow-flying birds. As a result, our analysis undoubtedly retained some PVs that were actually windborne and eliminated some that were actually birds.

The impact of misclassification depends on the analysis being done and the type of misclassification. When computing average bird densities, falsely including some windborne PVs is likely to have a very minor effect, since these PVs generally have very low reflectivity values (very close to zero on a linear scale; Fig. 3; Appendix S1: Fig. S1), while reflectivity values for bird PVs can be orders of magnitude larger. Falsely excluding some bird PVs will lead to density estimates that are too conservative by an amount that depends on the error rate. When analyzing direction and speed, falsely including some windborne PVs will lead to some measurements at the level of individual scans or elevation bins that are more

representative of wind velocity than bird velocity. However, these measurements will have correspondingly low bird densities, so weighting by bird density greatly mitigates this effect (Fig. 4). The impact of falsely excluding some bird PVs on direction and speed analyses is likely to be minor; the predominant effect will be the accuracy of the density measurements (discussed previously) used to weight average directions and speeds.

Overall, our methods of restricting scans to civil twilight periods, filtering PVs using wind velocities, and weighting statistical models by bird densities minimized the influence of windborne targets on our analysis, and we believe the final impact of such "contamination" on the broadscale patterns presented here is very minor. Our methods can be applied to the significant fraction of archived WSR-88D data for which improved classification based on the newer dual-polarization technology is not possible. However, caution is warranted when applying these methods at a finer-scale (in space and time): for example, an average density over a small number of PVs will be much more sensitive to PV level misclassification (see Appendix S1: Fig. S2). Further research is needed not only to confirm identities of biological targets in the atmosphere and improve classification techniques, but also to understand the sensitivity of analyses at different scales when applying different approaches for handling these targets.

Windborne targets were clearly widespread in our dataset. Although the identity of later season targets, which are clearly present (Fig. 2), is unknown, early season (e.g., August) windborne targets are certainly dominated by insects. Insect movements in the atmosphere can span large spatial and temporal extents (e.g., Westbrook et al. 2013). Windborne contamination peaks early in the night but continues in high proportions throughout the night with a secondary peak near dawn. This phenology, coupled with substantially high proportions in August and September, provides an opportunity for further investigation into optimal solutions to account for or to study insect movements in the atmosphere at large spatial and broad temporal scales.

Within-night variation in the density, direction, and speed of nocturnal migration

Infrequent, large movements may be a defining attribute of nocturnal bird migration (e.g., Ball 1952, Lowery and Newman 1966, Graber 1968, Nisbet 1969, Erni et al. 2002), but patterns of variation within nights have not been well studied. In particular, broad spatial and extended temporal studies of similarities in patterns of variation within nights are lacking. Our results generally agree with previous smaller scale studies that describe peak migration densities in the early part of the night after local twilight (Newman 1956, Lowery and Newman 1966, Farnsworth et al. 2004, Nebuloni et al. 2008). Similarities among studies in the nightly timing of migration presumably speaks mostly to the broad ranging effects of birds' diel cycles during migration period, with many individuals departing 30–45 min after local sunset and the largest numbers of birds aloft in the region occurring shortly thereafter (e.g., Hebrard 1971) and many migrants descending in the hours before and up to civil twilight.

Migration tracks observed in our study generally agree with patterns identified in previous studies (e.g., Drury and Keith 1977, Williams et al. 1977, 2001). However, these results extend our understanding by looking at migration on a substantially larger scale and for a longer period of seasonal migratory activity in the autumns of two years. Mean tracks ranged from south-southeast to south-southwest within nights, although birds at all radar stations showed substantial westerly shifts in direction over the course of the night. This directional shift was particularly pronounced mid-season, when the largest densities of migration occurred. Nightly changes in wind direction may explain some of this nightly variation, but such changes fail to account completely for the pronounced shifts exhibited by birds (see Horton et al. 2016 for additional explanation).

Wind direction shifted in a clockwise manner during the night for the September and October periods when bird migration was at its peak. On average, such a shift corresponded to a southeasterly wind heading becoming more southerly. This shift was much less dramatic during August and November. From August–October, migrants' tracks did not shift towards the south later in the night to meet more favorable winds, but rather birds flew more westerly tracks, even in August, when the average wind shift was negligible (Fig. 6). To what extent birds may be drifting with winds across our region is not clear, but these results suggest that mean migration tracks are not necessarily directly related to wind directions.

Whenever birds are migrating, they are subject to wind drift, whether partial or full (e.g., Green and Alerstam 2002). The prevailing winds from the west in the study region may drift birds that are primarily trying to go southwest farther to the east than desired, requiring regular correction. This is particularly important in the NEUS, where unchecked southbound migration will take birds over the Atlantic Ocean, a potentially deadly scenario for a songbird. If birds are drifted eastward toward the coast in the early hours of a movement, a correction to the west at the end of the evening may be a general compensation strategy. Recent studies of the behavior of birds that engage in migratory flights after sunrise (i.e., morning flight) highlighted a pattern in which migrants engaged in these flights after larger nocturnal movements and after the presence of stronger nocturnal crosswinds (Van Doren et al. 2015, Horton et al. 2016, Van Doren et al. 2016). Whether coastlines have a strong effect on orientation and its relationships with drift is still unclear, with evidence at smaller scales supporting consistent patterns of passerine (Nilsson et al. 2014) and waterfowl (O'Neal et al. 2014) movements regardless of whether birds are near coastlines. Our

results suggest that average movements in parallel to or away from coastal areas in the NEUS may be a common feature of late-night nocturnal migration. We do not know whether this is a strong preference to avoid water crossing or a result of intended headings of migrants destined for locations overland.

Mean groundspeeds showed generally similar patterns among nights in early and mid-season, with an early nightly peak. November exhibited a different pattern, with a peak just after nightfall. These late-season groundspeeds also exhibited the greatest within-night range from maximum to minimum speed. Airspeed patterns did not follow those of groundspeeds, instead increasingly rapidly during the first half of the night and then either increasing or decreasing depending on time of season. Several mechanisms could explain these patterns. First, migration strategies may force a diversity of birds to make choices, and these strategies may require faster travel during certain portions of the night. Birds may travel faster at certain points of the night to reach appropriate stopover habitat and maintain some degree of fidelity to an efficient route to their proximate and ultimate destinations. Our results suggest that increasing nightly airspeeds correspond to nightly periods when increasing numbers of birds are actively engaged in transit and sustained flight, and during a seasonal period when the largest numbers of birds are moving. An alternative explanation for within-season variability in airspeeds could be the changing species composition of nocturnally migrating birds. For example, there is an increased prevalence of waterfowl during the late season period (e.g., see Poole 2005) that are departing before sunset (after which groundspeeds are highest and declining) and leaving different locations in the region and of large flights of early morning pre-dawn diurnal migrants (e.g., blackbirds, Dolbeer 1978; finches, Middleton 1978, Wootton 1996). Variability in wind speeds does not appear to be fully responsible for the patterns apparent for migrating birds' speeds. Further analysis of winds relative to birds' intended directions of travel (e.g., the calculation of tailwinds) will be necessary to shed further light on this question. However, such an analysis would require accounting for the systematic and complex temporal variation in migration directions revealed here and is beyond the scope of this paper.

Among-night variation in the density, direction, and speed of nocturnal migration

Mid-September to mid-October was the period with peak densities of nocturnally migrating birds across the region, with substantially lower densities early and especially late in the season. Additionally, noticeably lower densities occurred at Boston, Massachusetts, USA, for the entirety of the fall season, strikingly so compared to the remainder of the stations. Several related factors may cause night-to-night variation in bird density over the season in our region (see Appendix S1: Fig. S3). Species migrate at different times and have widely different population sizes and breeding distributions, resulting in the observed changes in density over the course of the season and from night to night. Several hundred species regularly pass through the northeastern USA each fall, and their distributions in space and time are not uniform. Additionally, local and regional meteorology relates to nightly changes in migration densities (Able 1973, Richardson 1990, Dokter et al. 2013, Smolinsky et al. 2013). The NEUS experiences a diversity of meteorological conditions in the fall, and the regular passages of cyclonic storms and frontal boundaries likely govern the dynamics of nightly changes in bird densities.

Directions of travel also varied systematically through the season. Mean tracks were southwesterly over much of the season. An easterly shift at the very end corresponded to low densities of birds, but we have less confidence in the importance of this pattern and others at the tails of the season. Shifts in migration tracks did not correspond closely to shifts in wind directions, suggesting that wind direction shifts alone were not responsible for seasonal changes in migration tracks.

Much of this variation across the fall season presumably results from species-specific differences in migration timing, routes, and destinations. Earlier season migrants include species with trans-oceanic routes, and our data probably capture some birds migrating close to the coast and then departing over water, in addition to some proportion of trans-oceanic migrants that are making their way to the coast (La Sorte et al. 2016). These long-distance migrants include species departing over the Atlantic Ocean for South America, such as Blackpoll Warbler (*Setophaga striata*; see DeLuca et al. 2015) and Bobolink (*Dolichonyx oryzivorus*), or for the West Indies, such as Black-throated Blue Warbler (*Setophaga caerulescens*) and Cape May Warbler (*Setophaga tigrina*; e.g., Richardson 1976, McClintock et al. 1978, Larkin et al. 1979, Amos 1991, Nisbet et al. 1995, Renfrew et al. 2013). Targets over Boston, Massachusetts, USA, showed an average track that took birds offshore to the south over the Atlantic, probably including some of these species. Migrants over Portland, Maine, and Brookhaven, New York, USA, moved along more southwesterly tracks, taking birds overland and largely parallel to coastlines rather than across open water. These two stations, as well as other, inland stations appear to be overflown largely by short-distance migrants that move primarily overland within the USA or toward Central American destinations likely comprise the densities of birds moving generally southwest across the region. These shorter distance migrants may include species departing to the southwest overland for Central America, such as Yellow-bellied Flycatcher (*Empidonax flaviventris*) and Rose-breasted Grosbeak (*Pheucticus ludovicianus*; e.g., Russell 2005), and species departing to the southwest overland for the southeastern USA, such as Ruby-crowned Kinglet (*Regulus calendula*) and White-throated Sparrow (*Zonotrichia albicollis*; e.g., Robbins et al. 1989, Stouffer

and Dwyer 2003). The differences in timing of these movements and their relationships with seasonal and nightly directional shifts are beyond the scope of the present study, but future work is underway to assess these relationships.

Groundspeeds and airspeeds varied in somewhat different ways through the fall, although both increased through the season. As with seasonal changes in the direction of travel, changes in speeds among nights may represent changes in the species and their preferred directions of travel through the fall season. Larger bodied birds generally fly faster (Alerstam et al. 2007), and higher airspeeds may correspond to more migrating large-bodied birds. The distinct oscillation of groundspeeds coincided with cyclic changes in wind direction (and thus tailwinds) through the fall associated with frontal passages. However, a trend of increasing groundspeed was also evident. Higher groundspeeds were likely due both to generally increasing wind speeds, but also increasing airspeeds. Increasing airspeeds later in the season, especially through the month of October, may correspond to increasing proportions of larger and faster-flying birds, such as waterfowl and waterbirds (Pennycuick et al. 2013). The drop in airspeeds in November coincides with low migrant densities aloft and may not reflect true variation in bird speeds.

Variation among radar stations

Recent research using the same surveillance radars to describe stopover ecology of migrants may help explain the differences in average densities of birds that we found among sites. On the 59 nights when the largest densities of birds were moving across our region, the strongest positive correlations in bird densities were among northern inland stations and southern coastal stations. Buler and Dawson (2014) found significant stopover areas near the coast between Cape Cod, Massachusetts, and New York, New York, USA. That study also found that some of the highest mean bird densities and lowest levels of daily variability in densities occurred in eastern Connecticut and Rhode Island, USA, and to a lesser extent in southeastern Massachusetts, areas sampled in part by the Boston, Massachusetts, radar. Our correlations (Fig. 8) suggest that numbers of birds, which presumably use the same cues across a geographic area when deciding when to migrate at a particular time, overfly stations from Boston to the south along the coast. However, farther north along the coast at Portland, Maine, and across inland sites migrants appear to be moving in the largest numbers on different nights. These results suggest that in the northeastern USA, migrants are either traveling a coastal path from around Boston to the south or an inland path oriented along and inland from the Appalachian Mountains. Prevailing migration tracks were consistent with this notion, being strongly southwesterly at Portland, Maine, more so than at any other station, taking birds away from the Boston area.

Boston, Massachusetts, had the lowest densities of nocturnally migrating birds, suggesting that (1) numbers of birds using the transatlantic strategy do so in lower densities relative to densities of other migrating birds with different strategies or in a manner not well sampled by weather surveillance radar and (2) numbers of non-transatlantic migrants at Boston relative to such numbers at other stations were substantially lower. Additionally, birds may fly under the beam as they pass Boston (a 37.5 km radius from the Boston, Massachusetts, station barely reaches the Rhode Island coast and its stopover sites, with the beam height approximately 115–735 m above the ground) and move into more favorable habitat during the course of stopover periods (e.g., in morning flight, Van Doren et al. 2015, 2016; concentrations of birds in higher quality stopover habitat during the day, Faaborg et al. 2010, Wolfe et al. 2014). We also found an order of magnitude difference in bird densities between Boston, Massachusetts, and Brookhaven, New York, presumably highlighting the exodus of birds from Buler and Dawson's important stopover hotspots that eventually appears at Brookhaven, New York. Birds flying below the Boston radar's beam and moving toward any coastal stopover locations along the Connecticut and Rhode Island coasts would not appear on Boston's scans but instead appear on subsequent nights as targets on the Brookhaven scans, as the birds continued their migration. Whether this phenomenon represents this scenario or another, such as unquantified (and undetected because of the temporal duration of our study) diurnal movements of birds into stopover habitats, is beyond the scope of this study.

Application and future research

The results presented in this paper illustrate the potential for studying bird migration at very large scales made possible through interdisciplinary collaborations. By automating large parts of the processing of data from radar imagery (e.g., Sheldon et al. 2013), future analyses could expand to continental scales, substantially increasing the scope over that of previous studies (Lowery and Newman 1966, Gauthreaux et al. 2003). Further efficiency can still be gained over our methods, most notably by developing methods for initial screening of radar images for precipitation, a task for which we used human screening. The quantity of radar imagery available is massive: we estimate there are well over 100 million archived volume scans from some individual WSR-88D sites, and across the USA on a single night approximately 15 000 scans are produced nationwide.

Although the goal of this paper was to describe general patterns of variation in migration, substantial additional variation exists within and among nights and across seasons (e.g., Bagg et al. 1950, Richardson 1990, Erni et al. 2002). Determining the causes of this variation, particularly investigating the differences in migrants' responses to weather across local and regional scales, will

hopefully allow us to forecast times and locations of peak migration. For example, the strong correlations in densities among some radar stations could represent station-to-station hand offs related to migration paths and regional weather systems. The ability to make accurate forecasts would meet fundamental conservation-related needs. Flight safety for commercial air traffic and operational safety for military training exercises could be improved with additional knowledge of the spatial and temporal distribution of nocturnal migrants. Such data could also inform industrial and municipal activities: for example, when best to extinguish artificial lighting on buildings and other structures to avoid or minimize nocturnal migrant collisions; whether there is an appropriate window of time during a night, or during a migration season, to avoid activities like gas flaring or wind turbine operation; or if certain geographic areas are more likely to consistently pose a greater risk of migrants' collisions with structures because particularly large numbers of birds pass over those areas at night. Our results suggest that one period to target for conservation and mitigation measures may be the first half of nights during October, as these are the periods when the greatest numbers of birds are aloft. The effects of longer term changes in weather may also be addressed with the aid of data from weather radar (e.g., Frick et al. 2012).

Recent studies (Frick et al. 2012, Kelly et al. 2012, Buler and Dawson 2014) have shown the utility of weather radar information for understanding where and when animals land or depart, rather than when they are in active, long-distance flight. From the perspective of habitat conservation, and particularly conservation that targets important stopover habitats, more knowledge of traffic between and connections among sites would be invaluable. Acquiring this type of information would fill substantial information gaps for periods when birds' distributions are labile, as distinct from periods with greater stationarity, such as breeding and wintering periods (e.g., Runge et al. 2014).

A final area in which we see the potential for expanded research is in identifying the species of the birds detected by radar. In the future, some of this information may be available from newer, dual-polarization weather radar (Doviak et al. 2000, Seo et al. 2015); however, even this information would need to be corroborated by ground-based studies. In North America, we see the potential for combining radar-based information on the nights with heavy migration in combination with changes in numbers and identities of birds from ground-based surveys from the eBird program (Sullivan et al. 2014) in order to infer which species were flying in previous nights.

Conclusions

In this paper, we have shown that weather radar data, processed through a series of steps that minimize the influence of windborne targets and using newly created automated steps, can yield data about the migration of birds across wide regions and over entire migration seasons. We have described regional, seasonal, and nightly variation in the density, direction, and speeds of migrating birds from these data, and found that, in general, our study region represents an area over which migrant birds followed qualitatively similar strategies. However, we have also identified consistent quantitative differences both among sites within the region and through the season. We hypothesize that these differences are largely caused by differences in the species of bird traveling through the region on different routes (with some species departing from coastal sites for long over-water journeys to the Caribbean and South America) and at different times in the fall period. Further use of data from weather radar will have multiple applications both for basic research and conservation of migrants.

Acknowledgments

We thank Garrett Bernstein, Sidney Gauthreaux, Marshall Iliff, Frank La Sorte, Cecilia Nilsson, Amanda Rodewald, Ken Rosenberg, Brian Sullivan, Kevin Webb, Chris Wood, and two anonymous reviewers for extensive constructive comments and criticism. Grants from National Science Foundation (IIS-1125098), Leon Levy Foundation, and Wolf Creek Foundation supported this research.

Literature Cited

Alerstam, T., and A. Hedenström. 1998. The development of bird migration theory. Journal of Avian Biology 29:343–369.

Alerstam, T., M. Rosén, J. Bäckman, P. G. P. Ericson, and O. Hellgren. 2007. Flight speeds among bird species: allometric and phylogenetic effects. PLoS Biology 8:e197.

Alerstam, T., J. W. Chapman, J. Backman, A. D. Smith, H. Karlsson, C. Nilsson, D. R. Reynolds, H. G. Klaassen, and J. K. Hill. 2011. Convergent patterns of long-distance nocturnal migration in noctuid moths and passerine birds. Proceedings of the Royal Society B 278:3074–3080.

Amos, E. J. R. 1991. A Guide to the Birds of Bermuda. Privately published.

Bagg, A. M., W. W. H. Gunn, D. S. Miller, J. T. Nichols, W. Smith, and F. P. Wolfarth. 1950. Barometric pressure-patterns and spring bird migration. The Wilson Bulletin 62:5–19.

Ball, S. C. 1952. Fall bird migration of the Gaspé Peninsula. Peabody Museum of Natural History Yale University Bulletin 7:211 pp.

Bech, J., A. Magaldi, B. Codina and J. Lorente. 2012. Effects of anomalous propagation conditions on weather radar observations, Doppler Radar Observations – Weather Radar, Wind Profiler, Ionospheric Radar, and Other Advanced Applications, Dr. Joan Bech, editor. ISBN: 978-953-51-0496-4, InTech, doi:10.5772/38172. Available from: http://www.intechopen.com/books/doppler-radar-observations-weather-radar-wind-profiler-ionospheric-radar-and-other-advanced-applications/effects-of-anomalous-propagation-conditions-on-weather-radar-observations

Benjamini, Y., and Y. Hochberg. 1995. Controlling the false discovery rate: a practical and powerful approach to multiple testing. Journal of the Royal Statistical Society Series B (Methodological) 57:289–300.

Bridge, E. S., et al. 2011. Technology on the move: recent and forthcoming innovations for tracking migratory birds. BioScience 61:689–698.

Buler, J. J., and D. K. Dawson. 2014. Radar analysis of fall bird migration stopover sites in the northeastern US. The Condor 116:357–370.

Buler, J. J., and R. H. Diehl. 2009. Quantifying bird density during migratory stopover using weather surveillance radar. IEEE Transactions on Geoscience and Remote Sensing 8:2741–2751.

Buler, J. J., L. A. Randall, J. P. Fleskes, W. C. Jr Barrow, T. Bogart, and D. Kluver. 2012. Mapping wintering waterfowl distributions using weather surveillance radar. PLoS One 7:e41571.

Chapman, J. W., V. A. Drake, and D. R. Reynolds. 2011. Recent insights from radar studies of insect flight. Annual Review of Entomology 56:337–356.

Chilson, P. B., W. F. Frick, P. M. Stepanian, J. R. Shipley, T. H. Kunz, and J. F. Kelly. 2012. Estimating animal densities in the aerosphere using weather radar: to Z or not to Z? Ecosphere 3:art72.

Crum, T. D., and R. L. Alberty. 1993. The WSR-88D and the WSR-88D operational support facility. Bulletin of the American Meteorological Society 74:1669–1687.

Crum, T. D., R. L. Alberty, and D. W. Burgess. 1993. Recording, archiving, and using WSR-88D data. Bulletin of the American Meteorological Society 74:645–653.

DeLuca, W. V., B. K. Woodworth, C. C. Rimmer, P. P. Marra, P. D. Taylor, K. P. McFarland, S. A. Mackenzie, and D. R. Norris. 2015. Transoceanic migration by a 12 g songbird. Biology Letters 11:20141045.

Dokter, A. M., F. Liechti, H. Stark, L. Delobbe, P. Tabary, and I. Holleman. 2011. Bird migration flight altitudes studied by a network of operational weather radars. Journal of The Royal Society Interface 8:30–43.

Dokter, A. M., J. Shamoun-Baranes, M. U. Kemp, S. Tijm, and I. Holleman. 2013. High altitude bird migration at temperate latitudes: a synoptic perspective on wind assistance. PLoS One 8(1):e52300.

Dolbeer, R. A. 1978. Movement and migration patterns of Red-winged Blackbirds: a continental overview. Bird-Banding 49:17–34.

Doviak, R., and D. Zrnic. 1993. Doppler radar and weather observations. Academic Press, San Diego, CA.

Doviak, R. J., V. Bringi, A. Ryzhkov, A. Zahrai, and D. Zrnic. 2000. Considerations for polarimetric upgrades to operational WSR-88D radars. Journal of Atmospheric and Oceanic Technology 17:257–278.

Drake, V. A. 2014. Estimation of unbiased insect densities and density profiles with vertically pointing entomological radars. International Journal of Remote Sensing 35:4630–4654.

Erni, B., F. Liechti, L. G. Underhill, and B. Bruderer. 2002. Wind and rain govern the intensity of nocturnal bird migration in central Europe: a log-linear regression analysis. Ardea 90:155–166.

Faaborg, J., R. T. Holmes, A. D. Anders, K. L. Bildstein, K. M. Dugger, S. A. Gauthreaux, P. Heglund, K. A. Hobson, A. E. Jahn, D. H. Johnson, S. C. Latta, D. J. Levey, P. P. Marra, C. L. Merkord, E. Nol, S. I. Rothstein, T. W. Sherry, T. S. Sillett, F. R. Thompson, and N. Warnock. 2010. Conserving migratory land birds in the New World: do we know enough? Ecological Applications 20:398–418. doi:10.1890/09-0397.1

Farnsworth, A., S. A. Jr Gauthreaux, and D. E. Van Blaricom. 2004. A comparison of nocturnal call counts of migrating birds and reflectivity measurements on Doppler radar. Journal of Avian Biology 35:365–369.

Frank, A. L. S., D. Fink, W. M. Hochachka, and S. Kelling. 2016. Convergence of broad-scale migration strategies in terrestrial birds. Proceedings of the Royal Society B 283:20152588. doi:10.1098/rspb.2015.2588. Published 20 January 2016

Frick, W., P. M. Stepanian, J. F. Kelly, K. W. Howard, C. M. Kuster, T. H. Kunz, and P. B. Chilson. 2012. Climate and weather impact timing of emergence of bats. PLoS One 7:e42737.

Gauthreaux, S. A. Jr. 1969. A portable ceilometer technique for studying low-level nocturnal migration. Bird-Banding 40:309–320.

Gauthreaux, S. A. 1971. A radar and direct visual study of passerine spring migration in southern Louisiana. The Auk 88:343–365.

Gauthreaux, S. A. Jr, and J. W. Livingston. 2006. Monitoring bird migration with a fixed-beam radar and a thermal-imaging camera. Journal of Field Ornithology 77:319–328.

Gauthreaux, S. A.Jr, C. Belser and D. Van Blaricom. 2003. Using a network of WSR-88D weather surveillance radars to define patterns of bird migration at large spatial scales. Pages 335–346 *in* P. Berthold, E. Gwinner, and E. Sonnenschein, editors. Avian Migration. Springer-Verlag, Berlin.

Gauthreaux, S. A., J. W. Livingston, and C. G. Belser. 2008. Detection and discrimination of fauna in the aerosphere using Doppler weather surveillance radar. Integrative and Comparative Biology 48:12–23.

Graber, R. R. 1968. Nocturnal migration in Illinois—different points of view. The Wilson Bulletin 80:36–71.

Hebrard, J. J. 1971. The nightly initiation of passerine migration in spring: a direct visual study. Ibis 113:8–18.

Horn, J. W., and T. H. Kunz. 2008. Analyzing NEXRAD Doppler radar images to assess nightly dispersal patterns and population trends in Brazilian free-tailed bats (*Tadarida brasiliensis*). Integrative and Comparative Biology 48:24–39.

Horton, K. G., B. M. Van Doren, P. M. Stepanian, W. M. Hochachka, A. Farnsworth, and J. F. Kelly. 2016. Nocturnally migrating songbirds drift when they can and compensate when they must. Scientific Reports 6:21249. http://doi.org/10.1038/srep21249

Irvine, J. 2013. ScanLabeler. http://web.engr.oregonstate.edu/~irvine/scanlabeler.

Jahn, A. E., D. J. Levey, V. R. Cueto, J. Pinto Ledezma, D. T. Tuero, J. W. Fox, and D. Masson. 2013. Long-distance bird migration within South America revealed by light-level geolocators. The Auk 130:223–229.

Johnson, C. G. 1969. Migration and dispersal of insects by flight. Methuen, London.

Jones, T. A., and S. A. Christopher. 2009. Injection heights of biomass burning debris estimated from WSR-88D radar observations. IEEE Transactions on Geoscience and Remote Sensing 47:2599–2605.

Jones, T. A., S. A. Christopher, and W. Petersen. 2009. Dual-polarization radar characteristics of an apartment fire. Journal of Atmospheric and Oceanic Technology 26:2257–2269.

Kelly, J. F., J. R. Shipley, P. B. Chilson, K. W. Howard, W. F. Frick, and T. H. Kunz. 2012. Quantifying animal phenology in the aerosphere at a continental scale using NEXRAD weather radars. Ecosphere 3:1–9.

Kemp, M. U., J. Shamoun-Baranes, A. M. Dokter, E. van Loon, and W. Bouten. 2013. The influence of weather on the flight altitude of nocturnal migrants in mid-latitudes. Ibis 155:734–749.

Kerlinger, P., J. L. Gehring, W. P. Erickson, R. Curry, A. Jain, and J. Guarnaccia. 2010. Night migrant fatalities and

obstruction lighting at wind turbines in North America. The Wilson Journal of Ornithology 122:744–754.
Krauel, J. J., J. K. Westbrook, and G. F. McCracken. 2015. Weather-driven dynamics in a dual-migrant system: moths and bats. Journal of Animal Ecology 84:604–614.
Krueger, A. J., and R. A. Minzner. 1976. A mid-latitude ozone model for the 1976 U.S. Standard Atmosphere. Journal of Geophysical Research 81(24):4477–4481.
Larkin, R. P. 1991. Flight speeds observed with radar, a correction: slow "birds" are insects. Behavioral Ecology and Sociobiology 29:221–224.
Larkin, R. P., and R. H. Diehl. 2012. Radar techniques for wildlife biology. Pages 319–335 *in* C. E. Braun, editor. Techniques for wildlife investigations and management. Seventh edition. Wildlife Society, Bethesda, MD.
Larkin, R. P., D. R. Griffin, J. R. Torre-Bueno, and J. Teal. 1979. Radar observations of bird migration over the western North Atlantic Ocean. Behavioral Ecology and Sociobiology 4:225–264.
Loss, S. R., T. Will, and P. P. Marra. 2013. Estimates of bird collision mortality at wind facilities in the contiguous United States. Biological Conservation 168:201–209.
Loss, S. R., T. Will, S. S. Loss, and P. P. Marra. 2014. Bird-building collisions in the United States: estimates of annual mortality and species vulnerability. The Condor 116:8–23.
Lowery, G. H. Jr, and R. J. Newman. 1966. A continent wide view of bird migration on four nights in October. The Auk 83:547–586.
MATLAB and Statistics Toolbox Release. 2013b. 2013. The MathWorks Inc, Natick, Massachusetts, USA.
McClintock, C. P., T. C. Williams, and J. M. Teal. 1978. Autumnal bird migration observed from ships in the western North Atlantic Ocean. Bird-Banding 49:262–277.
McCracken, G. F., E. H. Gillam, J. K. Westbrook, Y. Lee, M. L. Jensen, and B. B. Balsley. 2008. Brazilian free-tailed bats (*T. brasiliensis*: Molossidae, Chiroptera) at high altitude: links to migratory insect populations. Integrative and Comparative Biology 48:107–118.
McKinnon, E. A., K. C. Fraser, and B. J. Stutchbury. 2013. New discoveries in landbird migration using geolocators, and a flight plan for the future. The Auk 130:211–222.
Mesinger, F., et al. 2006. North American regional reanalysis. Bulletin of the American Meteorological Society 87:343–360.
Middleton, A. L. A. 1978. The annual cycle of the American Goldfinch. Condor 80:401–406.
Minzner, R. A. 1977. The 1976 standard atmosphere and its relationship to earlier standards. Reviews of Geophysics 15:375–384.
National Climatic Data Center, NESDIS, NOAA, U.S. Department of Commerce. "NEXRAD LEVEL II (DSI-6500 through DSI-6899)" http://www.ncdc.noaa.gov/oa/radar/radarresources.html. Accessed 2 January 2014.
Nebuloni, R., C. Capsoni, and V. Vigorita. 2008. Quantifying bird migration by a high-resolution weather radar. IEEE Transactions on Geoscience and Remote Sensing 46:1867–1875.
Newman, R. J. 1956. Hour to hour variation in the volume of nocturnal migration in autumn. Ph.D. Dissertation. Louisiana State University, Baton Rouge, LA.
Nilsson, C., J. Bäckman, and T. Alerstam. 2014. Are flight paths of nocturnal songbird migrants influenced by local coastlines at a peninsula? Current Zoology 60:660–669.
Nisbet, I. C. T. 1969. A migration wave observed by moon watching and at banding stations. Bird Banding 40:243–252.
Nisbet, I. C., D. B. McNair, W. Post, and T. C. Williams. 1995. Transoceanic migration of the Blackpoll Warbler: summary of scientific evidence and response to criticisms by Murray. Journal of Field Ornithology 66:612–622.
O'Neal, B. J., J. D. Stafford, and R. P. Larkin. 2015. Migrating ducks in inland North America ignore major rivers as leading lines. Ibis 157:154–161. doi: 10.1111/ibi.12193
Pennycuick, C. J., S. Åkesson, and A. Hedenström. 2013. Air speeds of migrating birds observed by ornithodolite and compared with predictions from flight theory. Journal of The Royal Society Interface 10:20130419.
Poole, A. (editor). 2005. The Birds of North America Online. Cornell Laboratory of Ornithology, Ithaca, NY. http://bna.birds.cornell.edu/BNA/.
R Core Team 2014. R: A language and environment for statistical computing. R Foundation for Statistical Computing, Vienna, Austria. ISBN 3-900051-07-0. http://www.R-project.org/.
Renfrew, R. B., D. Kim, N. Perlut, J. Fox, J. Smith, and P. P. Marra. 2013. Phenological matching across hemispheres in a long-distance migratory bird. Diversity and Distributions 19:1008–1019.
Richardson, W. J. 1976. Autumn migration over Puerto Rico and the western Atlantic: a radar study. Ibis 118:09–332.
Richardson, W. J. 1990. Timing of bird migration in relation to weather: updated review. Pages 78–101 *in* E. Gwinner, editor. Bird migration. Springer-Verlag, Berlin Heidelberg.
Robbins, C. S., J. R. Sauer, R. S. Greenberg, and S. Droege. 1989. Population declines in North American birds that migrate to the Neotropics. Proceedings of the National Academy of Sciences 86:658–7662.
Runge, C. A., T. G. Martin, H. P. Possingham, S. G. Willis, and R. A. Fuller. 2014. Conserving mobile species. Frontiers in Ecology and the Environment 12:395–402.
Russell, R. W. 2005. Interactions between migrating birds and offshore oil and gas platforms in the northern Gulf of Mexico: Final Report. U.S. Department of the Interior, Minerals Management Service, Gulf of Mexico OCS Region, New Orleans, LA. OCS Study MMS 2005-009, 348 pp.
Russell, R. W., and J. W. Wilson. 1997. Radar-observed "Fine Lines" in the optically clear boundary layer: reflectivity contributions from aerial plankton and its predators. Boundary-Layer Meteorology 82:235–262.
Russell, R. W., M. L. May, K. L. Soltesz, and J. W. Fitzpatrick. 1998. Massive swarm migrations of dragonflies (Odonata) in eastern North America. The American Midland Naturalist 140:325–342.
Seo, B. C., W. F. Krajewski, and K. V. Mishra. 2015. Using the new dual-polarimetric capability of WSR-88D to eliminate anomalous propagation and wind turbine effects in radar-rainfall. Atmospheric Research 153:296–309.
Sheldon, D., A. Farnsworth, J. Irvine, B. Van Doren, K. Webb, T. G. Dietterich and S. Kelling. 2013. Approximate Bayesian inference for reconstructing velocities of migrating birds from weather radar. AAAI Conference on Artificial Intelligence, North America, June 2013. http://www.aaai.org/ocs/index.php/AAAI/AAAI13/paper/view/6468. Accessed 2-January-2014.
Smolinsky, J. A., R. H. Diehl, T. A. Radzio, D. K. Delaney, and F. R. Moore. 2013. Factors influencing the movement biology of migrant songbirds confronted with an ecological

barrier. Behavioral Ecology and Sociobiology 67:2041–2051.

Stouffer, P. C., and G. M. Dwyer. 2003. Sex-biased winter distribution and timing of migration of Hermit Thrushes (*Catharus guttatus*) in eastern North America. The Auk 120:836–847.

Van Doren, B. M., D. Sheldon, J. Geevarghese, W. M. Hochachka, and A. Farnsworth. 2015. Autumn morning flights of migrant songbirds in the northeastern United States are linked to nocturnal migration and winds aloft. The Auk 132:105–118.

Warning Decision Training Branch 2008. Quick Reference VCP Comparison Table for RPG itself. Mean and standard error correlations do not account for these identity correlations.

Westbrook, J. K., R. S. Eyster, and W. W. Wolf. 2013. WSR-88D doppler radar detection of corn earworm moth migration. International Journal of Biometeorology 58:931–940.

Wolfe, J. D., M. D. Johnson, and C. J. Ralph. 2014. Do Birds select habitat or food resources? Nearctic-neotropic migrants in northeastern Costa Rica. PLoS ONE 9:e86221.

Wolff, D. B. 2009. NASA's Radar Software Library (RSL) and RSL in IDL. In 34th Conference on Radar Meteorology, 5–9 October 2009, Williamsburg, Virginia, USA.

Wood, S. 2006. Generalized additive models: an introduction with R. CRC Press, Boca Raton, FL.

Wood, S. N. 2011. Fast stable restricted maximum likelihood and marginal likelihood estimation of semiparametric generalized linear models. Journal of the Royal Statistical Society: Series B (Statistical Methodology) 73:3–36.

Wootton, J. T. 1996. Purple Finch (*Haemorhous purpureus*), The Birds of North America Online. A. Poole, editor. Cornell Lab of Ornithology, Ithaca. Retrieved from the Birds of North America Online: http://bna.birds.cornell.edu/bna/species/208. http://dx.doi.org/10.2173/bna.208.

Supporting Information

Additional supporting information may be found in the online version of this article at http://onlinelibrary.wiley.com/doi/10.1890/15-0023/suppinfo

Data Availability

Data associated with this paper have been deposited in Dryad: http://dx.doi.org/10.5061/dryad.17209